AIP | Applied Physics Letters

Shear waves in vegetal tissues at ultrasonic frequencies

M. D. Fariñas, D. Sancho-Knapik, J. J. Peguero-Pina, E. Gil-Pelegrín, and T. E. Gómez Álvarez-Arenas

Citation: Applied Physics Letters **102**, 103702 (2013); doi: 10.1063/1.4795785
View online: http://dx.doi.org/10.1063/1.4795785
View Table of Contents: http://scitation.aip.org/content/aip/journal/apl/102/10?ver=pdfcov
Published by the AIP Publishing

Shear waves in vegetal tissues at ultrasonic frequencies

M. D. Fariñas,[1] D. Sancho-Knapik,[2] J. J. Peguero-Pina,[2] E. Gil-Pelegrín,[2] and T. E. Gómez Álvarez-Arenas[1,a)]
[1]*UMEDIA research group, Spanish National Research Council, CSIC, Madrid, Spain*
[2]*Unidad de Recursos Forestales, CITA, Gobierno de Aragón, Zaragoza, Spain*

(Received 12 November 2012; accepted 5 March 2013; published online 15 March 2013)

Shear waves are investigated in leaves of two plant species using air-coupled ultrasound. Magnitude and phase spectra of the transmission coefficient around the first two orders of the thickness resonances (normal and oblique incidence) have been measured. A bilayer acoustic model for plant leaves (comprising the palisade parenchyma and the spongy mesophyll) is proposed to extract, from measured spectra, properties of these tissues like: velocity and attenuation of longitudinal and shear waves and hence Young modulus, rigidity modulus, and Poisson's ratio. Elastic moduli values are typical of cellular solids and both, shear and longitudinal waves exhibit classical viscoelastic losses. Influence of leaf water content is also analyzed. © *2013 American Institute of Physics*. [http://dx.doi.org/10.1063/1.4795785]

Generation and propagation of shear waves in animal tissues and organs have already been used by different characterization, test, and imaging techniques. They are commonly used in the transient elastography, the supersonic shear wave elastography, and the elastography using acoustic radiation force.[1,2] A large number of medical applications are currently being developed and investigated based on the fact that mechanical properties of soft tissues change depending on the state of diseases like breast cancer, hepatic fibrosis, or thrombosis. The working frequency is typically between 50 and 1000 Hz. Young modulus of these soft tissues use to be very low (between 17 Pa for fat and up to 300 MPa for the Aquilles' tendon[3]).

For vegetal tissues, there is an increasing interest in the study of tissues' elasticity: understanding the interaction of the plant with the external mechanical stimuli,[4] mathematical modeling of the role of internal mechanical tensions in cell proliferation and plant patterns formation,[5] manufacturing of synthetic nano-composites using plant primary cell walls,[6] and non-invasive sensing of plants watering needs.[7] Unlike animal cells, vegetal cells are surrounded by a cell wall. In the past, this wall was viewed as an inanimate rigid scaffold, but it is now recognized as a dynamic structure that plays an important role in controlling the development of the plant and the adaptation to the environment.[8,9] One of its functions is to withstand the osmotic pressure of the cell. So, the combination of cell pressure and cell wall strength contributes to the whole rigidity of plants. Cell walls may differ in function and in composition. The walls surrounding growing and dividing plant cells must provide mechanical strength but must also expand to allow the cell to grow and divide. Once the cell has ceased to grow, a much thicker and stronger wall may then develop.[9] In general, cell wall accounts for most of the carbohydrate in biomass. In addition, it may have a major impact on human life, as it is a major component of wood, a source of nutrition for livestock, and account for the bulk of renewable biomass that can be converted to fuel out of a plant. These features suggest that it might be possible to observe the propagation of shear waves in plant tissues at ultrasonic frequencies and that this can provide valuable information, which may have significant economic implications.

Some ultrasonic techniques using longitudinal waves have been applied in the past to study plant leaves.[10,11] More recently, air-coupled ultrasound and normal incidence have been used to excite and sense thickness resonances in plant leaves to obtain in a non invasive and a nondestructive way valuable information about plant status.[7,12,13] Although a similar technique, but using oblique incidence, has been conventionally used to generate and sense shear waves in other materials,[14] no evidence of the appearance of shear waves at ultrasonic frequencies in plant leaves has been previously reported for some species.[7] The purpose of this paper is to study shear waves in plant leaves using a broadband air-coupled ultrasonic technique and normal and oblique incidence. Properties of the leaf tissues are extracted from the measured spectra using a bilayer acoustic model.

Three pairs of air-coupled and wide band ultrasonic transducers were used in a through transmission experimental set-up (transmitter-receiver separation of 45 mm), center frequencies are 0.25, 0.70, and 1.00 MHz, usable bandwidths 0.15–0.35 MHz, 0.35–0.90 MHz, and 0.60–1.50 MHz, and sensitivities −25 dB, −29 dB, and −35 dB, respectively. Transmitter transducer is driven by a Panametrics 5058 pulser. The received signal is amplified 40 dB, high-pass filtered (0.03 MHz), and digitized by a Tektronix 7054 digital oscilloscope. Angle of incidence is controlled by a goniometer. Magnitude and phase spectra of the transmission coefficient are measured for all leaves varying the angle of incidence from 0° to 40° in steps of 5° (see Figs. 1–3). At normal incidence, shear wave generation does not take place and transmission coefficient is defined by the pattern of the thickness resonances, which is produced by the longitudinal wave and the finite leaf dimensions. As the angle of incidence increases, part of the particle displacement produced by the incident ultrasound field on the leaf surface takes place on the plane of the leaf, shear displacements are

a)Author to whom correspondence should be addressed. Electronic mail: tgomez@ia.cetef.csic.es.

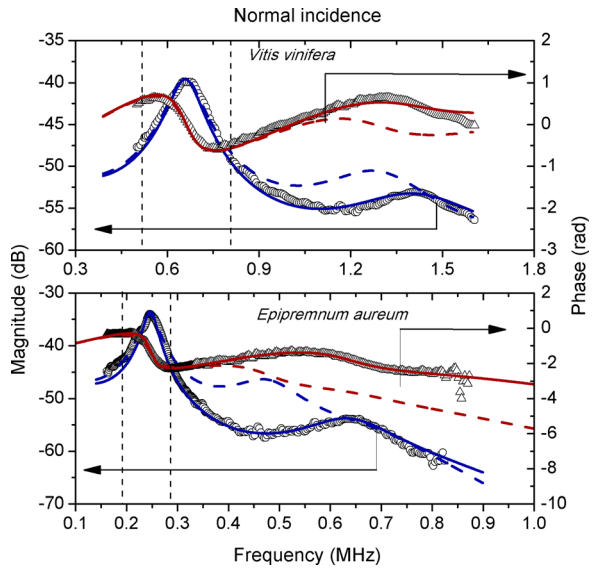

FIG. 1. Magnitude and phase spectra of the transmission coefficient at normal incidence. ○ and △: measured magnitude and phase spectra, respectively. Dashed line: theoretical predictions of the one-layer model (*V. vinifera*: $v^L = 341$ m/s, $\rho = 866$ kg/m^3, $t = 256$ μm, $\alpha_0^L = 991$ Np/m, $f_{res} = 659$ kHz, and $n = 1.75$. *E. aureum*: $v^L = 194$ m/s, $\rho = 894$ kg/m^3, $t = 391$ μm, $\alpha_0^L = 590$ Np/m, $f_{res} = 246$ kHz, and $nL = 1.75$). Solid line: theoretical predictions of the bilayer model (*V. vinifera*: $v_{PP}^L = 450$ m/s, $v_{SM}^L = 300$ m/s, $\rho_{PP} = 952$ kg/m^3, $\rho_{SM} = 779$ kg/m^3, $t_{PP} = t_{SM} = 128$ μm, $\alpha_{PP0}^L = \alpha_{SM0}^L = 940$ Np/m, and $nL = 1.8$. *E. aureum:* $v_{PP}^L = 400$ m/s, $v_{SM}^L = 175$ m/s, $\rho_{PP} = 1254$ kg/m^3, $\rho_{SM} = 444$ kg/m^3, $t_{PP} = t_{SM} = 195$ μm, $\alpha_{PP0}^L = \alpha_{SM0}^L = 451$ Np/m, and $nL = 2$).

generated, and consequently, mode conversion takes place and shear waves are generated. As the angle of incidence increases, more energy is coupled into the shear mode. This shear wave also reverberates within the leaf and produces a

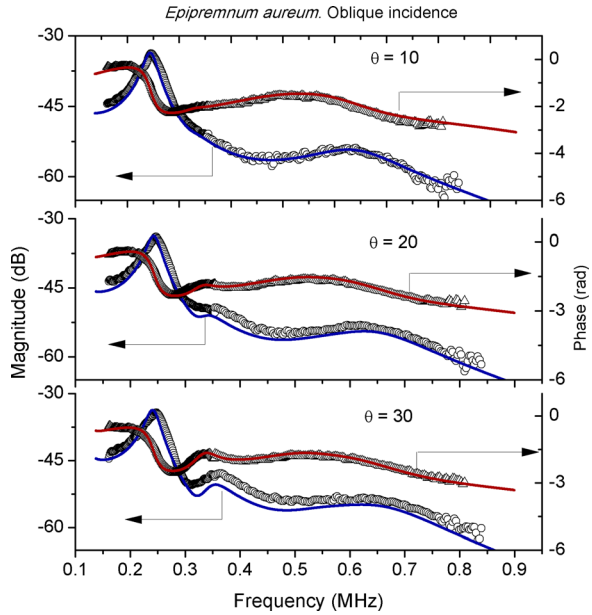

FIG. 2. Magnitude and phase spectra of the transmission coefficient versus frequency for a *E. aureum* leaf at three angles of incidence (10°, 20°, and 30°). ○ and △: measured magnitude and phase spectra, respectively. Solid lines (blue and red): calculated magnitude and phase spectra using the bilayer model, respectively. Data for the calculations are in Fig. 1 caption together with the following shear wave data: Poisson's ratio = 0.33 (this implies $v_{PP}^{SH} = 200$ m/s and $v_{SM}^{SH} = 88$ m/s), $\alpha_0^{SH} = 924$ Np/m, and $nSH = 2$. Longitudinal thickness resonance appears at 248 kHz and the interference with the shear wave resonance appear (for incidence angle > 15°) close to 300 kHz.

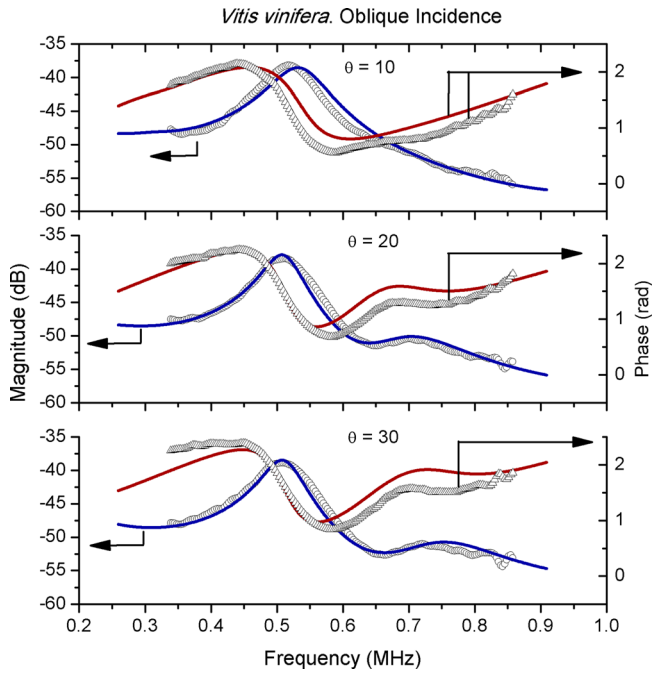

FIG. 3. Magnitude and phase spectra of the transmission coefficient versus frequency for a *V. vinifera* leaf at three angles of incidence (10°, 20°, and 30°). ○ and △: measured magnitude and phase spectra, respectively. Solid lines (blue and red): calculated magnitude and phase spectra using the bilayer model, respectively. Data for the calculations are $t_{PP} = t_{SM} = 147$ μm, $f_{res} = 531$ kHz, $v_{PP}^L = 500$ m/s, $v_{SM}^L = 274$ m/s, $\rho_{PP} = 950$ kg/m^3, $\rho_{SM} = 680$ kg/m^3, $\alpha_0^L = 750$ Np/m, $nL = 2$, Poisson's ratio = 0.34 (this implies $v_{PP}^{SH} = 245$ m/s, $v_{SM}^{SH} = 134$ m/s), $\alpha_0^{SH} = 1500$ Np/m, and $nSH = 2$. The interference with the shear wave resonance appears (for incidence angle > 15°) close to 650 kHz.

pattern of thickness resonances. As long as measurements are taken at an angle below the limit angle for longitudinal waves, this shear wave resonances overlaps to the pattern of thickness resonances due to the longitudinal wave (see Figs. 2 and 3), so what we observe is the overlap or interference of these two patterns of thickness resonances: longitudinal and shear (see also Ref. 14).

For comparison purposes, longitudinal and shear wave velocities were also obtained from conventional time of flight measurements using a through transmission technique with direct contact and commercial shear-wave and longitudinal-wave transducers (0.5 MHz, Panametrics). To efficiently couple shear-wave transducer to the leaves, a commercial shear wave coupling gel was used.

Leaves from different species were tested, in many cases, no shear waves were observed (e.g., *Platanus hispanica*, *Ligustrum lucidum*, *Prunus laurocerasus,* and immature—spring time—*Vitis vinifera* leaves). This can be attributed to a very high attenuation coefficient of shear waves in these leaves. However, in some other cases, shear waves were clearly seen. This paper focuses on leaves of *Epipremnum aureum* and mature (summer time) leaves of *V. vinifera,* where shear waves were observed. Another reason to select these species is that they correspond to two extreme cases from the point of view of the bilayer acoustic model: the two layers of *E. aureum* leaves are strongly different while they are very similar for *V. vinifera* leaves. Ten leaves of *V. vinifera* were collected and preserved according to the procedure in Ref. 7. Ten

leaves of *E. aureum* were measured directly from the plant without cutting them.

To theoretically analyze the presence of shear waves in the transmission coefficient spectra, the analysis cannot be limited to the vicinity of the first thickness resonance but must include a larger frequency window.[7,15] This requires that the layered structure of the leaf must be considered, in other words, the one-layer effective model used in previous works cannot be used now (see Fig. 1).

The mathematical model considered here for plant leaves consists of a stack of two layers of different tissues (bilayer model). The first layer (PP-layer) comprises the upper epidermis and the palisade parenchyma (PP) while the second one (SM-layer) comprises the spongy mesophyll (SM) and the lower epidermis. The cells of the parenchyma tissues are densely packed together: they can be thought of as a pressurized, liquid-filled closed-cell foam,[9] with an effective density close to the density of its main constituents: water ($1000\,kg/m^3$), cellulose ($1500\,kg/m^3$), ligning ($1300\,kg/m^3$), and wax ($950\,kg/m^3$). The SM layer can also be considered a cellular material, but with a relatively higher porosity and open-cell structure for it must allow the gaseous interchange with the surrounding air. Thicknesses of these two layers are considered equal,[16,17] and also the attenuation coefficient and the Poisson's ratio.

First, the one-layer model is employed to extract effective leaf properties from measurements at normal incidence in the vicinity of the first resonance as explained in Ref. 12. In all cases, it is assumed that velocity does not change with the frequency (f) and that attenuation coefficient (α^L and α^{SH}, for longitudinal and shear waves, respectively) follows a power law as it has been done in the past for a large number of porous materials and biological tissues[18]

$$\begin{aligned} \alpha^L &= \alpha_0^L (f/f_{res})^{nL}, \\ \alpha^{SH} &= \alpha_0^{SH} (f/f_{res})^{nSH}, \end{aligned} \tag{1}$$

where f_{res} is the frequency of the first thickness resonance.

Figure 1 shows measurements of the transmission coefficient spectra at normal incidence. Leaf effective properties obtained using the one layer model[13] (see Fig. 1 caption) are used as initial values for the bilayer model. Then, we only allow to change velocity and density of the PP and the SM layers (they become stepwise more different, i.e., anisotropy between layers is increased) until the fitting of the theoretically calculated transmission coefficient into the experimental data over the whole frequency range reaches an optimum value. Results are also shown in Fig. 1.

Once these data are determined, the magnitude and the phase spectra of the transmission coefficient at oblique incidence are theoretically calculated using the set of parameters obtained at normal incidence and only changing the Poisson ratio, from -1 to 0.5 in steps of 0.01. Negative Poisson's ratio values were considered because such values have been previously reported for some vegetal tissues.[19] The purpose is to theoretically reproduce the frequency location of the shear wave interference. Once this is achieved, shear wave attenuation is changed until the calculated amplitude of this interference matches the experimental value. Results for three angles of incidence are shown in Figures 2 and 3, the appearance of the shear wave is clear for incidence angles beyond 10°. Although there is little information about the Poisson ratio in vegetal tissues, obtained values here (0.33 and 0.34) agree with available estimations: 0.28 (lignin), 0.18–0.4 (onion epidermis), and 0.23–0.5 (parenchyma tissues).[5,20–23] The fact that nL and nSH are close to 2 confirm that the main source of losses have a classical viscoelastic origin with the condition that $\omega\tau \ll 1$, where τ is a relaxation time that characterizes the medium and ω the angular frequency.

TABLE I. Longitudinal, v^L, and shear, v^{SH}, wave velocities (m/s) in the leaves obtained by the two different experimental methods.

	Gel coupling		Air-coupled spectroscopy	
	v^L	v^{SH}	$\langle v^L \rangle$	$\langle v^{SH} \rangle$
E. aureum	320 ± 27	180 ± 18	290 ± 15	145 ± 10
V. vinifera	460 ± 50	155 ± 17	390 ± 15	190 ± 10

With the purpose to confirm these results, longitudinal and shear wave velocities were measured using a direct contact, through transmission technique at 0.5 MHz. In this case, the results are affected by a relatively large uncertainty due to the irregularities of the leaf surfaces and the difficulty to efficiently attach the transducers to them. Ten leaves of each species were measured at three different points. Averaged data and standard deviations are shown in Table I. For comparison purposes, average values $\left(\langle v^L \rangle = (v^L_{PP} + v^L_{SM})/2 \text{ and } \langle v^{SH} \rangle = (v^{SH}_{PP} + v^{SH}_{SM})/2\right)$. obtained by the air-coupled technique and the bilayer model are also shown.

From these data, elastic moduli can be worked out, results are summarized in Table II.

These values are similar to data reported before for vegetable tissues (e.g., Young modulus of 8–19 MPa for parenchyma cells, 2–22 MPa for aerenchyma and collenchyma cells, respectively,[9,19,24] and 50–200 MPa for Quercus leaves;[21] and modulus of rigidity between 2 and 22 MPa (Ref. 25)). At normal or high turgor pressures, the cell walls are taut, and deformation is dominated by stretching of the cell walls. The Young's modulus of the parenchyma tissue (E_{tissue}) is then directly proportional to its relative density (which is equivalent to the volume fraction of solids: ϕ_s)[9]

$$E_{tissue} \propto E_{cw}\phi_s, \tag{2}$$

where E_{cw} is Young modulus of the cell wall. So, measured E_{tissue} values can be used to compare the microstructure of different parenchyma tissues or parenchyma tissues from

TABLE II. Elastic moduli of the leaf tissues.

Tissue		E (MPa)	G (MPa)
V. vinifera	PP	150 ± 5	60 ± 3
	SM	30 ± 3	12 ± 1
E. aureum	PP	135 ± 5	50 ± 2
	SM	9 ± 1	3 ± 0.5

different species by comparing the value of the proportionally constants in Eq. (2).

It is worthwhile noting that the appearance of shear waves in *V. vinifera* strongly depends on the leaf degree of development. For leaves collected at spring time, $\alpha_0^L > 1000$ Np/m, there is no evidence of the shear waves. On the contrary, for leaves collected during summer and fall, $\alpha_0^L \approx 750$ Np/m, the shear wave is clearly detected. This can be produced by the further evolution and stiffening of the cell wall produced when the leaf growth is finished.[8,9]

Finally, the influence of leaf water content was studied. Towards this end, leaf weight and magnitude and phase spectra of the transmission coefficient at an incidence angle of 30° were measured in leaves cut at full saturation and then left to dry at room conditions. Measurements were taken every 3 min during 3 h. Once finished, the leaves were fully dried in a stove at 70° during 24 h to obtain the leaf dry weight and then the leaf relative water content (RWC).[17] The variation with RWC in the measured longitudinal thickness resonance frequency (f_{res}) and in the other PP-layer parameters extracted from the measurements is shown in Figure 4. Variation in f_{res} with RWC follows a sigmoid behavior as reported before for other species measured at normal incidence[15] and the point of turgor loss can be determined from the location of the point of inflection: RWC_0. The exact location of this point of inflection is calculated by fitting the logistic curve (Eq. (3)) into the experimental data ($RWC_0 = 0.935$).

$$y = y^0 + (y^F - y^0) \Big/ \left(1 + \left((RWC/RWC_0)\right)^p\right), \qquad (3)$$

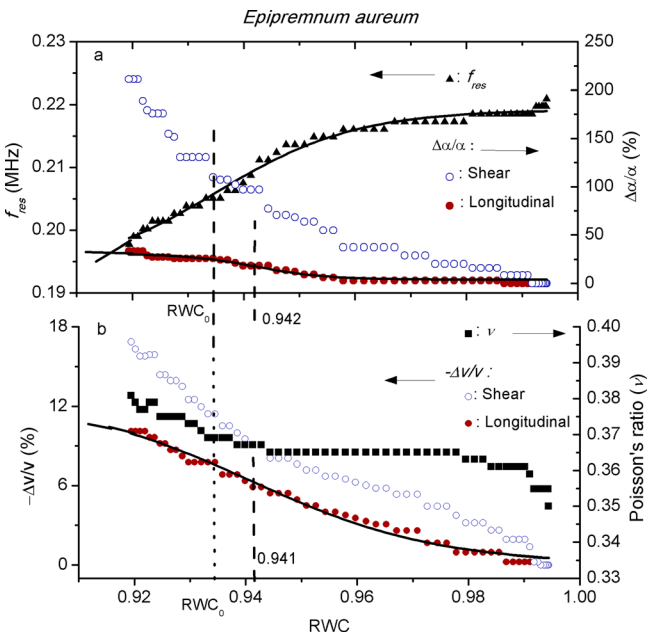

FIG. 4. Variation in the properties of the PP-layer of a *E. aureum* leaf during dehydration. Solid lines: fitting of the logistic function (Eq. (3)) into the corresponding experimental data. Vertical dashed lines indicate the location of the point of inflection of the solid-line curves. Fig. 4(a) ▲: Variation in f_{res} (left vertical axis) with RWC; Relative variation in the attenuation coefficient (right vertical axis) with RWC. ○ (blue): $\Delta\alpha^L/\alpha_0^L$ and ● (red): $\Delta\alpha^{SH}/\alpha_0^{SH}$. Fig. 4(b) ■: Variation in the Poisson's ratio (right vertical axis) with RWC; Relative variation in the velocity (left vertical axis) with RWC. ○ (blue): $\Delta v_{PP}^{SH}/v_{PP}^{SH}$ and ● (red): $\Delta v_{PP}^{L}/v_{PP}^{L}$.

where superscripts *0* and *F* denote the full water saturation and the final (dry) states, respectively. v_{PP}^L and α_{PP}^L vs. RWC also follow a sigmoid variation, and it is possible to fit the logistic curve (Eq. (3)) into these measurements, obtained points of inflection are also shown in Fig. 4 and are very close to RWC_0.

Shear properties (v_{PP}^{SH} and α_{PP}^{SH}) and Poisson's ratio does not follow a sigmoid evolution with RWC. Attenuation continues increasing beyond the turgor loss point while velocity keeps on decreasing. Another feature found in shear waves, and not in longitudinal waves, is the initial high rate of variation in v_{PP}^{SH} with RWC. These features are reflected in the variation in the Poisson's ratio with RWC that presents two transitions one at the very beginning of the desiccation process ($RWC = 0.99$) and the other close to RWC_0.

All these features can be explained by the overall loss of rigidity and the increase of compressibility in the vegetal tissues when water content is reduced due to the decay of the pressure of the cells against the cell wall: cell wall is no longer taut and deformation takes place by bending. In addition, it is observed that while the shear velocity keeps decreasing beyond the turgor loss point (and, hence, also *G*), the longitudinal velocity reaches a limit value (consequently, also the modulus of compressibility *K*: $v^L = \sqrt{(K + 4/3G)/\rho}$).

In summary, this work demonstrates the feasibility of propagate and detect shear waves in plant leaves in a completely non-invasive way using wideband air-coupled ultrasonic pulses and a bilayer model for the leaf to extract leaf parameters from measured spectra, and reveals the potential use of this technique to study the elasticity of the different vegetal tissues and their variations due to leaf development or to water content changes.

Financial support from Spanish MINECO through Project DPI 2011-22438 is acknowledged.

[1]L. S. Wilson, D. E. Robinson, and M. J. Dadd, Phys. Med. Biol. **45**(6), 1409 (2000).
[2]M. Tanter, J. Bercoff, A. Athanasiou, T. Deffieux, J.-L. Gennison, G. Montalvo, M. Muller, A. Tardivon, M. Fink, Ultrasound Med. Biol. **34**(9), 1373 (2008).
[3]I. Levental, P. C. Georges, and P. A. Janmey, Soft Matter **3**(3), 299 (2007).
[4]F. W. Telewski, Am. J. Bot. **93**(10), 1466 (2006).
[5]A. C. Newell and P. D. Shipman, J. Stat. Phys. **121**(5–6), 937 (2005); R. Kennaway, E. Coen, A. Green, and A. Bangham. PLoS Comput. Biol. **7**(6), e1002071 (2011).
[6]D. M. Bruce, R. N. Hobson, J. W. Farrent, and D. G. Hepworth, Composites, Part A **36**(11), 1486 (2005); A. P. Kumar, D. Depan, N. Singh Tomer, and R. P. Singh, Prog. Polym. Sci. **34**(6), 479 (2009).
[7]T. E. Gómez Álvarez-Arenas, D. Sancho-Knapik, J. J. Peguero-Pina, and E. Gil-Pelegrín, Appl. Phys. Lett. **95**(19), 193702 (2009); D. Sancho-Knapik, T. Gómez Álvarez-Arenas, J. J. Peguero-Pina, and E. Gil Pelegrín, J. Exp. Bot. **61**(5), 1385 (2010).
[8]D. J. Cosgrove, Nat. Rev. Mol. Cell Biol. **6**(11), 850 (2005).
[9]L. J. Gibson, J. R. Soc., Interface **9**(76), 2749 (2012).
[10]M. Fukuhara, Plant Sci. **162**(4), 521 (2002).
[11]P. S. Wilson and K. H. Dunton, J. Acoust. Soc. Am. **125**(4), 1951 (2009).
[12]D. Sancho-Knapik, T. G. Álvarez-Arenas, J. J. Peguero-Pina, V. Fernández, and E. Gil-Pelegrín, J. Exp. Bot. **62**(10), 3637 (2011).
[13]D. Sancho-Knapik, H. Calás, J. J. Peguero-Pina, A. Ramos Fernandez, E. Gil-Pelegrín, and T. E. Gómez Alvarez-Arenas, IEEE Trans. Ultrason. Ferroelect. Freq. Control **59**(2), 319 (2012).
[14]T. E. Gómez Álvarez-Arenas, F. Montero, M. Moner-Girona, E. Rodríguez, A. Roig, and E. Molins, Appl. Phys. Lett. **81**(7), 1198 (2002).

[15]T. E. Gómez Álvarez-Arenas, D. Sancho-Knapik, J. J. Peguero-Pina, and E. Gil Pelegrin, in *2009 IEEE International Ultrasonics Symposium, Rome* (2009), pp. 771–774.
[16]H. Toshoji, T. Katsumata, M. Takusagawa, Y. Yusa, and A. Sakai, Protoplasma **249**(3), 805 (2012).
[17]A. Ben Salem-Fnayou, B. Bouamama, A. Ghorbel, and A. Mliki, Microsc. Res. Tech. **74**(8), 756 (2011).
[18]T. Szabo, J. Acoust. Soc. Am. **96**, 491 (1994).
[19]K. J. Niklas, *Plant Biomechanics* (The University of Chicago Press, London, 1992).
[20]T. J. Brodribb and N. M. Holbrook, Plant Physiol. **137**, 1139 (2005).
[21]T. Saito, K. Soga, T. Hoson, and I. Terashima, Plant Cell Physiol. **47**(6), 715 (2006).
[22]C. Wei, P. M. Lintilhac, and J. J. Tanguay, Plant Physiol. **126**(3), 1129 (2001).
[23]E. Vanstreels, M. C. Alamar, B. E. Verlinden, A. Enninghorst, J. K. A. Loodts, E. Tijskens, H. Ramon, and B. M. Nicolaï, Postharvest Biol. Technol. **37**(2), 163 (2005).
[24]J. Blahovec, J. Mater. Sci. **23**(10), 3588 (1988).
[25]I. Burgert, Am. J. Bot. **93**(10), 1391 (2006).